Inseparable Waveform Synthesis in Joint Communications and Radar via Spatial-Frequency Spectrum

Husheng Li
The University of Tennessee, Knoxville, TN, USA
hli31@utk.edu

***Abstract*—Joint communications and radar (JCR), which use the same waveform for both functions, provide an efficient scheme of spectrum access and find various applications in practice such as autonomous driving. A convenient signaling framework is the orthogonal frequency-division multiplexing and multi-in-multi-out (OFDM-MIMO) structure, which corresponds to the spatial-frequency spectrum resulted from high-dimensional Fourier transform. The key challenge of JCR is how to resolve the interest conflict between communications and radar sensing, when they share the same waveform in an inseparable manner. The corresponding trade-off is formulated as constrained optimization problems for the cases of analog and digital beamformings. Numerical results show that the proposed schemes are effective in the spatial-frequency spectrum management and achieve good performance trade-offs between communications and radar sensing.**

I. Introduction

Communications and radar are two major applications of electromagnetic (EM) waves. In the history, they were developed, designed and operated independently, although they share many common characteristics and benefit from the design principles of each other. In recent years, due to the congestion of frequency spectrum, particularly in the sub-6GHz band, there have been significant studies on the integration of communications and radar. One effective approach is independent operation with the mitigation of mutual interference for co-existence. A more efficient scheme is the dual-function radar and communications (DFRC) [1]–[3], in which communication and radar signals are linearly superimposed to each other and can be separated in time (time multiplexing), frequency (frequency multiplexing), or space (beamforming). In this paper, we consider a tighter integration, called joint communications and radar (JCR), in which the two functions share the same waveform in an inseparable manner (namely any piece of radio resource is not dedicated to a single function). A simple illustrative example is given as follows: a JCR transceiver sends out EM waves, over which the data packets are modulated; the communication receiver intercepts the EM wave through its aperture and then decodes the information; meanwhile, the EM waves reflected by targets are received by the JCR transceiver and used for inferring the information of the targets. The two functions are realized in the forward and backward propagations of the same EM wave.

For integrating communications and radar in the same hardware and waveform, it is beneficial to incorporate common signaling techniques. Although the frequency modulation continuous waveform (FMCW) is popular in modern radar systems, it is difficult to embed high-throughput data in the FMCW waveform. A better scheme is to use the signaling framework of orthogonal frequency -division multiplexing (OFDM) plus multi-in-multi-output (MIMO), which have been studied in both communications and radar. In this paper, we also propose to use the framework of Fourier transform to analyze and design the OFDM-MIMO JCR, namely exploiting the Fourier transform (thus the spatial-frequency spectrum) relationship between the source charge and generated fields.

A critical step for the design of JCR is to identify the conflict between communications and radar, which results in the corresponding performance trade-off. In this paper, we focus on the following two conflicts that exist in systems with analog and digital beamformings, respectively:

- Conflicting preference on power spectral density (PSD): The performances of communications and radar ranging are given by [4], [5]
$$C = \int_B \log_2\left(1+\frac{S(f)}{N_0}\right)df, \text{ and } \delta d \geq \frac{c}{\beta\sqrt{\frac{2E}{N_0}}}, \quad (1)$$
where $\beta^2 = \frac{\int_B f^2 S(f)df}{\int_B S(f)df}$ is called the effective bandwidth, C is the communication channel capacity, E is the pulse energy, N_0 is the noise PSD, B is the frequency band, δd is the ranging error, c is the light speed, and $S(f)$ is the signal PSD. Then, in frequency-flat channels, communications prefer a uniform PSD, while radar likes a PSD with more power in the higher frequency band (as FMCW radar does). A trade-off is needed between the preferences of communications and radar.
- Conflicting preference on signal subspaces: For the digital beamforming case, communications desire to place

power in the subspaces of greater eigenvalue of the channel matrix; meanwhile, multi-target radar prefers to enhance the signature vectors of different targets. The allocation of power over the subspaces needs to be Pareto efficient[1] for the two objectives.

The remainder of this paper is organized as follows. The researches related to this paper are introduced and compared in Section II. The system model and Fourier framework are introduced in Section III. Then, the waveforms are optimized in the contexts of analog and digital beamformings, in Sections IV and V, respectively. The corresponding numerical results are provided in Section VI. Finally the conclusions are drawn in Section VII.

II. Related Work

In this section, we introduce the existing studies related to this paper. Comprehensive surveys on the coexistence or DFRC of communications and radar can be found in [1], [2], [7], [8]. Waveform design has been a long-lasting research topic in radar systems [9], which becomes a major issue in JCR. In many existing studies, the DFRC waveform is sent by the same hardware using a linear superimposition of traditional communication and radar signals, which can be separated by time, frequency or space. Although the spatial separation of the two functions via beamforming [1]–[3] achieves higher spectral efficiency than the time/frequency separation, due to the reuse of the frequency, the mutual interference of communication and radar beams is still significant in practice [10], [11]. There are some nonlinear and inseparable designs of shared waveform: the fractional Fourier transform is employed for the waveform design [12]; in the millimeter wave band, the joint waveform design has been analyzed from the signal processing perspective in [13]. However, these studies did not exploit the spatial-frequency spectrum, and failed to analyze the conflict between communications and radar.

III. System Model

In this section, we introduce the system model used in this paper. In particular, we adopt the Fourier transform relationship between the source and EM field, which will be used in the subsequent sections.

A. System

We consider a JCR transceiver, whose center is set as the coordinate origin. The JCR transceiver is equipped with N antennas, whose positions are not specified unless mentioned otherwise. We assume that a multi-carrier structure, the same as in OFDM systems, is used for the transmit waveform. The subcarrier frequencies are given by $f_k = f_0 + (k-1)\delta f$, $k = 1, ..., K$, where f_0 is the initial frequency, δf is the spacing of subcarriers, and K is the number of subcarriers. The corresponding wavenumbers are denoted by $\{k_i\}_{i=1,...,K}$. The time is slotted; within each time slot the baseband signals can be considered as constants. We denote by $X_{nk}(t)$ the complex baseband signal sent at the k-th subcarrier and the n-th antenna at time slot t. The complex waveform within one OFDM symbol period is given by

$$s_n(t) = \sum_{k=1}^{K} X_{nk} \exp(j(2\pi f_k t + \phi_{kn})), \tag{2}$$

where ϕ_{kn} is the corresponding phase. We assume that $\{X_{nk}\}_{nk}$ are quadrature amplitude modulation (QAM) symbols. The following two cases of spatial processing will be discussed in this paper:

- Analog beamforming: Each antenna sends the same baseband signal with shifted phases, namely $X_{nk} = X_k e^{j\phi_n}$.
- Digital beamforming: Different antennas may have arbitrary values of X_{nk}.

B. Fourier Framework

The Fourier transform relationship between the source charges and the corresponding EM fields is of key importance in the development of radar imaging. We adopt this framework and provide a brief introduction subsequently. Consider a region Ω of source charges harmonically oscillating with frequency f. The origin is within Ω. The charge density at position $\mathbf{r} \in \Omega$ is denoted by $\rho(\mathbf{r})$, which is complex. Consider the field at position $\mathbf{r}'$, which is far away from the source charges such that the field is a far field. Under the assumption of far field, the field is determined by the Fresnel approximation (Chapter 4.2 in [14])

$$E(\mathbf{r}') \approx \frac{e^{-jk|\mathbf{r}'|}}{\|\mathbf{r}'\|^2} \int_{\Omega} \rho(\mathbf{r}) e^{-jk\mathbf{r}'\cdot\mathbf{r}} d\mathbf{r}, \tag{3}$$

where k is the wavenumber of the EM wave.

We define the wavevector $\mathbf{k}' = k\mathbf{r}'$ and define the normalized field x as

$$x(\mathbf{k}') = E(\mathbf{r}') e^{jk|\mathbf{r}'|} \|\mathbf{r}'\|^2. \tag{4}$$

By assuming that the approximation in (3) is exact, we have

$$x(\mathbf{k}') = \int_{\Omega} \rho(\mathbf{r}) e^{-jk\mathbf{k}'\cdot\mathbf{r}} d\mathbf{r}, \tag{5}$$

which indicates that the normalized far field and the source charge form a Fourier transform pair.

[1]Pareto efficiency, or Pareto optimality, is a state at which resources cannot be reallocated to make one individual better off without making at least one individual worse off [6].

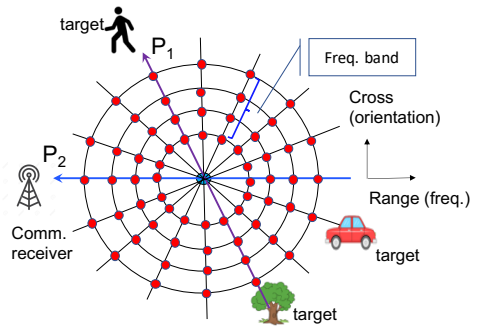

Fig. 1. An illustration of the spatial-frequency spectrum

IV. Field Optimization: Analog Beamforming

In this section, we discuss the case of analog beamforming, namely the inputs to all antennas are the same waveform, except for the amplitude and phase. Note that the beamforming in JCR has been discussed in [15]. In a contrast, communications and radar use different waveforms and are separated by distinct beams in [15], while the functions of communications and radar are inseparable in our proposed waveforms.

A. Fourier Formualtion

We first assume a continuous distribution $\rho_i(\cdot)$ of charges with harmonic oscillating frequency f_i in the region Ω of the JCR transceiver. The continuous charge distribution can then be approximated by multiple transmit antennas as spatial samples. Note that there are K distributions $\{\rho_i\}_{i=1,...,K}$, each corresponding to a subcarrier. Then, according to the Fourier relationship in (6), the field at wavevector $\mathbf{k}_i$ is given by

$$x_i(\mathbf{k}_i) = \mathcal{F}(\rho_i)(\mathbf{k}_i), \tag{6}$$

where $\mathcal{F}$ denotes the Fourier transform. Therefore, the fields resulted from the transmitted signal can be represented by a K-fold field $\{x_i(\mathbf{r})\}_{i=1,...,K}$. Now, we consider only the fields on the unit circle. Hence, the field is a function of the angle and frequency (wavenumber). The K-fold field, called the spatial-frequency spectrum, can be represented by the 2-dimensional lattice illustrated in Fig. 1. Each dot represents the field associated with the corresponding direction and wavenumber.

B. Waveform Design

For simplicity, we assume a communication beam and a radar sensing beam, as illustrated in Fig. 1. Moreover, we consider only the task of ranging for radar sensing. Then, the conflict between communications and radar consists of the power split and the different preferences of PSD.

1) Fixed Power Allocation: We first fix the power allocations to radar and communications, denoted by P_1 and P_2, respectively, and consider the two functions as two agents, whose utility functions are given by the sum channel capacity

$$U_c(P_1, P_2, \mathbf{x}) = \sum_{k=1}^{K} \log\left(1 + \frac{g_k P_2 x_k}{N_0}\right), \tag{7}$$

where $\{x_k\}_{i=k,...,K}$ are the power proportions on the subcarriers, $\{g_k\}_{k=1,...,K}$ are the channel gains of the subcarriers and N_0 is the noise power, and the approximated effective bandwidth (see Eq. (1)) of radar ranging

$$U_r(P_1, P_2, \mathbf{x}) = P_1 \sum_{k=1}^{K} f_k^2 x_k, \tag{8}$$

respectively, subject to the constraints $P_1 + P_2 = P$, $\sum_{k=1}^{K} x_k = 1$, and $P_i, x_k \geq 0$, $i = 1, 2, k = 1, ..., K$.

Then, we optimize the following linear combination:

$$\max_{\mathbf{x}} aU_c(P_1, P_2, \mathbf{x}) + (1-a)U_r(P_1, P_2, \mathbf{x}), \tag{9}$$

where $0 \leq a \leq 1$ is a weighting factor. By taking derivative with respect to x_k and consider the constraints, we have

$$aP_1 f_k^2 + \frac{1-a}{x_k + \frac{N_0}{g_k P_2}} = \lambda_0 + \lambda_k, \tag{10}$$

where λ_0 is the Lagrange multiplier for the constraint of total power, and λ_k is that of the constraint $x_k \geq 0$. When $x_k > 0$ and $\lambda_k = 0$, we have

$$x_k = \frac{1-a}{(\lambda_0 - aP_1 f_k^2)} - \frac{N_0}{g_k P_2}. \tag{11}$$

When $\frac{1-a}{\lambda_0 - aP_1 f_k^2} \leq \frac{N_0}{g_k P_2}$, we have $x_k = 0$. Thus, we observe that the optimal solution tends to allocate more power to x_k for greater k (namely higher frequency subcarrier). The preference is determined by the weighting factor a. When $a = 0$, the solution is the standard water-filling in communications.

We notice that (11) is similar to the conventional water-filling in multi-channel communications, except that the water surface increases with the frequency, as illustrated in Fig. 2.

2) Pareto Optimum: Recall that we have fixed the powers P_1, P_2 and the weighting factor a. However, it is not necessary for an arbitrary combination (P_1, P_2, a) and the corresponding optimal $\{x_k\}_{k=1,...,K}$ to be a Pareto optimum. We also need to check P_1 and P_2. Taking derivative for (9) with respect to P_1 and P_2, we have the equilibrium condition for P_1:

$$a \sum_{k=1}^{K} x_k f_k^2 = \lambda', \tag{12}$$

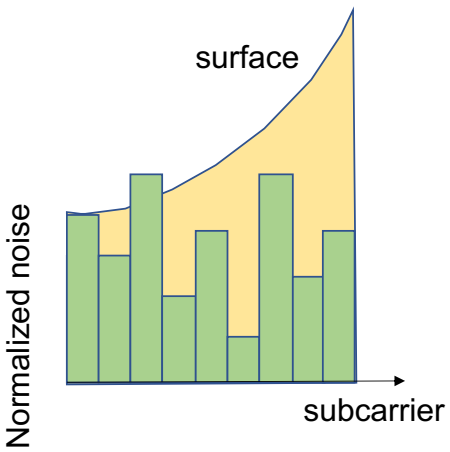

Fig. 2. Water filling with uneven surface

and the equilibrium condition for P_2:

$$(1-a)\sum_{k=1}^{K}\frac{\frac{g_k x_k}{N_0}}{1+\frac{g_k x_k P_2}{N_0}}=\lambda', \tag{13}$$

where λ' is the Lagrange multiplier of the constraint $P_1 + P_2 = P$. Therefore, the selection of weighting factor a should guarantee that the left hand sides of (12) and (13) are identical. We notice that the left hand side of (12) increases linearly with a and equals 0 when $a = 0$, while that of (13) equals 0 when $a = 1$. Therefore, there must exists an a (not necessarily unique) such that (12) and (13) are identical, thus guaranteeing the existence Pareto optimum.

It is unclear whether the left hand side of (13) decreases monotonically with a; if yes, the value of a making (12) and (13) identical is unique. To explore this, we rewrite (10) as

$$(1-a)\sum_{k=1}^{K}\frac{\frac{g_k P_2}{N_0}}{1+\frac{g_k x_k P_2}{N_0}}=\frac{1}{P_2}\sum_{k=1}^{K}x_k\left(\lambda_0-aP_1f_k^2\right). \tag{14}$$

Substituting (11) into the right hand side of (14), we obtain

$$\begin{aligned}&(1-a)\sum_{k=1}^{K}\frac{\frac{g_k P_2}{N_0}}{1+\frac{g_k x_k P_2}{N_0}}\\ =\;&\frac{K(1-a)}{P_2}-\frac{N_0}{P_2^2}\sum_{k=1}^{K}\frac{\lambda_0-aP_1f_k^2}{g_k},\end{aligned} \tag{15}$$

as an alternative expression for the left hand side of (13).

Taking derivative with respect to a, we have

$$\frac{d}{da}\left(\text{LHS of (13)}\right)=-\frac{K}{P_2}-\sum_{k=1}^{K}\frac{N_0}{g_k P_2^2}\left(\frac{d\lambda_0}{da}-P_1f_k^2\right). \tag{16}$$

The derivative $\frac{d\lambda_0}{da}$ is difficult to evaluate. However, we can verify that it is bounded. Therefore, for sufficiently small N_0, (16) is negative, thus making (13) decrease monotonically with a. Hence, for each pair P_1 and P_2, there is a unique a such that P_1, P_2 and the corresponding $\{x_k\}$ are Pareto optimal, when the SNR is sufficiently high.

V. Digital Beamforming: Multiple Targets

In this section we consider the case of sensing multiple targets, which are detected using the signature waveform of digital beamforming, while still transmitting to a single communication receiver. The performance of MIMO radar has been intensively studied. In this paper, we focus on the identifiability of multiple targets due to the MIMO structure, which has been studied in [16], [17]. This can be compared with the multiplexing in MIMO communications by providing independent channels. Due to the different linear structures in the communication and radar channels, the corresponding trade-off will be analyzed and achieved.

A. Signal Subspace

For the discrete antenna arrays and point target, the source is discrete in the space, thus resulting in the linear relationship between the transmitted signal and received signal (as N-dimensional vectors) at subcarrier i:

$$\mathbf{s}_i=\sum_{j=1}^{M}\psi_j\mathbf{S}_i(\mathbf{t}_j)\mathbf{w}_i, \tag{17}$$

where M (the number of targets), ψ_j (the scattering coefficient of target j), $\mathbf{w}$ is the vector of signals at the N transmitters and $\mathbf{t}_j$ (position of target j) are unknown, and the signature matrix $\mathbf{S}_i(\mathbf{t}_j)$ is given by

$$\mathbf{S}_i(\mathbf{t}_j)=\mathbf{u}_i(\mathbf{t}_j)\mathbf{v}_i^H(\mathbf{t}_j), \tag{18}$$

where $\mathbf{v}_i(\mathbf{t}_j)$ is the linear functional that maps the illumination source to the field at position $\mathbf{t}_j$, while $\mathbf{u}_i(\mathbf{t}_j)$ is the linear functional that maps from the field at position $\mathbf{t}_j$ to the received signal at the antenna.

When the signal reception reuses the transmit antennas, or the receive antennas are close to the transmit antennas, we have $\mathbf{u}_i = \mathbf{v}_i$. We call them signature waveforms. We further rewrite (17) as

$$\mathbf{s}_i=\bar{\mathbf{S}}_i\mathbf{x}_i,\qquad i=1,...,K, \tag{19}$$

where $\mathbf{S}_i$ is the signature matrix for subcarrier i:

$$\bar{\mathbf{S}}_i=\sum_{j=1}^{M}\mathbf{S}_i(\mathbf{t}_j)=\sum_{j=1}^{M}\psi_j\mathbf{v}_i^H(\mathbf{t}_j)\mathbf{v}_i(\mathbf{t}_j), \tag{20}$$

where we assume $M < N$. Notice that (20) is the spectral decomposition of $\bar{\mathbf{S}}_i$, where ψ_j is the eigenvalue and $\mathbf{v}_i(\mathbf{t}_j)$ is the orthogonal eigenvectors.

From the above analysis, we realize that, for each subcarrier i, the targets form a subspace $\{\mathbf{v}_i(\mathbf{t}_j)\}_{j=1,..,M}$. To enhance the performance of detecting the targets, it is desirable

to place the transmitted signal in the desired subspaces. When there are significantly many reflectors in the communication channel, such that the communication channel matrix is of high rank, the covariance matrix of transmit signal vector $\mathbf{w}$ needs to be designed using water-filling for the decoupled channels obtained by the singular value decomposition (SVD) of the channel matrix. More conflict between communications and radar could be incurred when the communication channel matrix is of low rank: the traditional water-filling will allocate power to a low-dimensional subspace, thus possibly nulling the signature vectors of many targets.

B. Power Allocation

Now we address the challenge of resolving the conflict in the power allocation in different signal subspaces.

1) Single Carrier Case: For a single carrier, we denote the signature vectors of targets by $\mathbf{v}_1$, ..., $\mathbf{v}_M$, where the subscript is used to indicate the target. The orthonormal eigenvectors of $\mathbf{H}\mathbf{H}^T$, where $\mathbf{H}$ is the communication channel matrix, are denoted by $\{\mathbf{z}_l\}_{l=1,...,N}$, while the corresponding eigenvalues are $\{g_i\}_{i=1,...,N}$. Note that some g_i's could be zero, if the rank of $\mathbf{H}$ is less than N.

For the single carrier case, we formulate the problem of power allocation as

$$\begin{aligned} & \max_{P_1,...,P_N} \sum_{j=1}^{N} \log\left(1+\frac{P_j g_j}{N_0}\right) \\ s.t. \quad & \sum_{j=1}^{N} V_{ij} P_j \geq \gamma, \forall i = 1, ..., M \\ & P_j \geq 0, \forall j = 1, ..., N \\ & P_1 + P_2 + ... + P_N = P, \end{aligned} \tag{21}$$

where $V_{ij} = |\mathbf{v}_i^T \mathbf{z}_j|^2$, P_i is the power placed on the singular vector $\mathbf{z}_i$, and γ is the performance threshold for the radar sensing. The solution is given by

$$P_j = \frac{1}{\lambda^c + \sum_{i=1}^{M} \lambda_i^r V_{ij} + \lambda_j^0} - \frac{N_0}{g_j}, \tag{22}$$

when $P_j \geq 0$, where λ^c, $\lambda_i^r \leq 0$ and $\lambda_j^0 \leq 0$ are the Langrange multipliers for the total power constraint, the radar performance constraint and the nonnegative power, respectively. When the powers $\{P_i\}_{i=1,...,N}$ are obtained, the powers $\{Q_i\}_{i=1,...,N}$ allocated to each antenna can be obtained from $\mathbf{p} = \mathbf{Z}\mathbf{q}$, where $\mathbf{p}$ and $\mathbf{q}$ are the vectors of powers allocated to different singular vectors and different antennas, respectively, and $\mathbf{Z} = (\mathbf{z}_1, ..., \mathbf{z}_N)$.

To obtain the Lagrange multipliers and thus the solution in (22), we begin from pure water filling for the communications by setting λ_i^r to be zero. Then, we increase the value of λ_i^r for the target whose performance deficiency is the maximal. This iteration will be repeated until convergence.

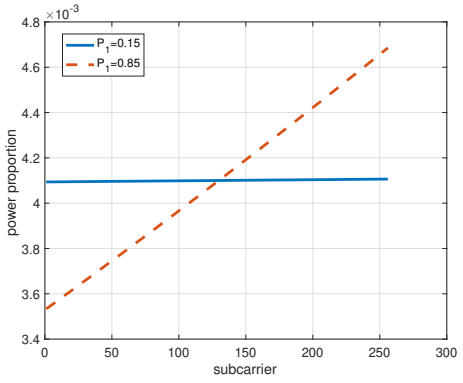

Fig. 3. Power allocation for different trade-offs in analog beamforming

2) Multicarrier Case: The above single-carrier case can be easily extended to multicarrier case. We simply have MN signature vectors and NK decoupled channels. The same optimization can be formulated for optimizing the NK transmit powers. The details of formulation are omitted due to the limited space.

VI. Numerical Results

In this section, we provide numerical simulation results for demonstrating the proposed algorithms.

A. Analog Beamforming

We first implemented the proposed algorithm of finding Pareto front. We consider the 60GHz band with 256 subcarriers and spacing of 1MHz. The noise PSD is -174dBm/Hz. We assume that both the target and communication receiver are 50 meters away. The path loss exponent is set to 3.5. The pulse duration is set to 100us. The transmit power is assumed to be 20mW. For simplicity, we assume that the communication channel is frequency-flat, namely the channel gains are identical for all subcarriers.

Figure 3 shows the power spectrum obtained from the water-filling, with $\frac{P_1}{P} = 0.15$ and $\frac{P_1}{P} = 0.85$. The corresponding weighting factor a is obtained at the Pareto optimum. We observe that the PSD is much flatter when P_1 is small, namely more emphasis is placed on communications, thus tending to the constant PSD desired by the communication task. Another observation is that, in both typical situations, the PSDs are approximately linear.

Figure 4 shows the trade-off curve between communications (channel capacity) and radar ranging (standard deviation of ranging error). Since the trade-off curve is the boundary of the feasible region of JCR, only the performance metrics in the right side of the curve can be achieved. We also observe that the communication performance saturates when the radar ranging error becomes substantial. The same saturation is observed for the radar ranging, when the communication

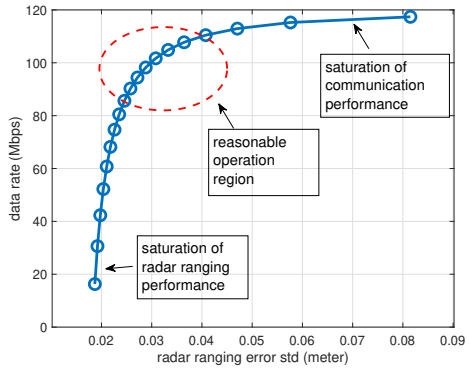

Fig. 4. Communication-ranging trade-off in analog beamforming

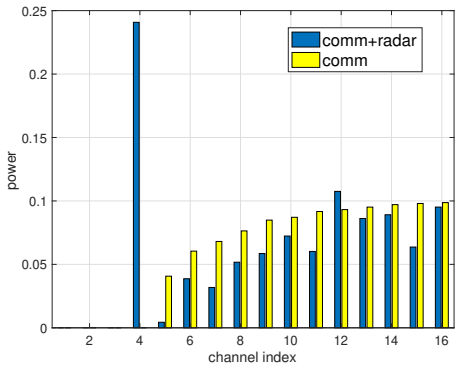

Fig. 5. Comparison of power allocations for pure communications and JCR

capacity significantly drops. Therefore, a reasonable operation region is the middle part of the curve, which is efficient for both communications and radar ranging.

B. Digital Beamforming

We also tested the case of multiple targets and sufficient reflectors in the communication channel, for the digital beamforming case. 16 transmit antennas are considered. A single carrier of 60GHz is assumed. We assume that the channel gains of the singular vectors of $\mathbf{H}$ satisfy the complex Gaussian distribution, and the targets are uniformly distributed on a circle of radius 100m. We consider a unit transmit power and assume that the received SNR is 5dB. In the optimization problem in (21), we set the threshold γ of radar received power to be 0.1.

In Fig. 5, we show the comparison between the power allocations (to the singular vectors of the channel matrix $\mathbf{H}$) for pure communications and JCR, respectively, in one realization of the communication channel and target positions. The indices of singular vectors are sorted in the order of increasing eigenvalues (channel power gains). We observe that the allocated power for pure communications increases with the index (thus the channel power gain) due to the water-filling. When radar sensing is taken into account, the power allocation is significantly changed. Particularly, in singular vector 4, the power allocation is substantially increased, due to the requirement of power along the signature vectors of the radar targets.

VII. Conclusions

In this paper, we have discussed JCR with inseparable waveforms, using OFDM-MIMO. A Fourier transform framework has been employed for the analysis and design. We have studied the power allocations in the contexts of analog and digital beamformings, respectively. Numerical simulations have been carried out for evaluating the performances and disclosing interesting discoveries in the proposed algorithms.

References

[1] B. Paul, A. R. Chiriyath, and D. W. Bliss, "Survey of rf communications and sensing convergence research," *IEEE Access*, vol. 5, pp. 252–270, 2016.

[2] F. Liu, C. Masouros, A. Petropulu, H. Griffiths, and L. Hanzo, "Joint radar and communication design: Applications, state-of-the-art, and the road ahead," *IEEE Transactions on Communications*, 2020.

[3] D. Ma, N. Shlezinger, T. Huang, Y. Liu, and Y. C. Eldar, "Joint radar-communications strategies for autonomous vehicles," *IEEE Signal Processing Magazine*, vol. 37, no. 4, pp. 85–97, 2020.

[4] T. M. Cover and J. A. Thomas, *Elements of Information Theory*. Wiley, 2006.

[5] M. I. Skolnik, *Introduction to Radar Systems (3rd edition)*. McGraw-Hill, 2001.

[6] R. B. Myerson, *Game Theory: Analysis of Conflict*. Harvard University Press, 1991.

[7] L. Han and K. Wu, "Joint wireless communication and radar sensing systems–state of the art and future prospects," *IET Microwaves, Antennas & Propagation*, vol. 7, no. 11, pp. 876–885, 2013.

[8] L. Zheng, M. Lops, Y. C. Eldar, and X. Wang, "Radar and communication co-existence: an overview," *arXiv preprint arXiv:1902.08676*, 2019.

[9] H. He, J. Li, and P. Stoica, *Waveform Design for Active Sensing Systems: A Computational Approach*. Cambridge University Press, 2012.

[10] D. W. Bliss and H. Govindosamy, *Adaptive Wireless Communications: MIMO Channels and Networks*. Cambridge University Press, 2011.

[11] K. W. Forsythe, "Utilizing waveform features for adaptive beamforming and direction finding with narrow-band signals," *Lincoln Laboratory Journal*, vol. 10, no. 2, pp. 99–126, 1997.

[12] D. Gaglione, C. Clemente, C. V. Ilioudis, A. R. Persico, I. K. Proudler, J. J. Soraghan, and A. Farina, "Waveform design for communicating radar systems using fractional fourier transform," *Digital Signal Processing*, vol. 80, pp. 57–69, 2018.

[13] K. V. Mishra, M. B. Shankar, V. Koivunen, B. Ottersten, and S. A. Vorobyov, "Toward millimeter-wave joint radar communications: A signal processing perspective," *IEEE Signal Processing Magazine*, vol. 36, no. 5, pp. 100–114, 2019.

[14] J. W. Goodman, *Introduction to Fourier Optics*. Roberts & Company Publisher, 2005.

[15] J. A. Zhang, X. Huang, Y. J. Guo, J. Yuan, and R. W. Heath Jr, "Multibeam for joint communication and sensing using steerable analog antenna arrays," *arXiv preprint arXiv:1810.04105*, 2018.

[16] J. Li, P. Stoica, L. Xu, and W. Roberts, "On parameter identifiability of mimo radar," *IEEE Signal Procss. Lett*, vol. 14, no. 2, pp. 968–971, 2007.

[17] J. Li and P. Stoica, *MIMO Radar Signal Processing*. Wiley, 2009.